Synthesis and Characterization of Kinked and Hyperbranched Carbazole/Fluorene-Based Copolymers

ARTICLE *in* MACROMOLECULES · SEPTEMBER 2006

Impact Factor: 5.8 · DOI: 10.1021/ma061770j

2 AUTHORS, INCLUDING:

Hong-Cheu Lin
National Chiao Tung University
155 PUBLICATIONS **2,437** CITATIONS

Synthesis and Characterization of Kinked and Hyperbranched Carbazole/Fluorene-Based Copolymers

Chung-Wen Wu and Hong-Cheu Lin*

Department of Materials Science and Engineering, National Chiao Tung University, Hsinchu, Taiwan (ROC)

Received August 4, 2006; Revised Manuscript Received August 25, 2006

ABSTRACT: To decrease the aggregation phenomena and improve the luminescent properties of polyfluorenes (PFs), a series of novel kinked and hyperbranched carbazole units were copolymerized by the Suzuki coupling polycondensation reaction to introduce disorder packing into the copolymer backbones. The thermal, photophysical, electrochemical, and electroluminescent properties of the copolymers were investigated. All of these polymers possess excellent thermal stability with onset decomposition temperatures at 407−466 °C and glass transition temperatures at 109−140 °C. Photoluminescent (PL) studies showed that these polymers were promising blue light-emitting materials, which exhibited high quantum efficiencies in solution and solid states. Long wavelength emissions at 500−600 nm, which were typical for PFs due to their self-aggregation in the solid state, were suppressed in these polymers. Annealing studies under air showed both improved thermal and photoluminescence stability of the polymers. It was proven that HOMO energy levels of the copolymers can be enlarged by increasing the carbazole content in the electrochemical measurements; hence, the hole injection was greatly enhanced. Pure-blue electroluminescence (EL) spectra with narrow fwhm (full width at the half-maximum) values (39−42 nm) and negligible low-energy excimer emission bands were successfully achieved, indicating that these copolymers could be good candidates for blue light-emitting materials.

Introduction

Over the past few years, polyfluorene (PF) derivatives have emerged as a promising class of blue-light-emitting conjugated polymers for use in polymer-based emissive displays because of high photoluminescent (PL) and electroluminescent (EL) yields as well as easy tunability of physical properties through chemical structure modification and copolymerization.[1] Some thorny problems associated with PFs are their tendencies of forming aggregates, excimers, and ketone defects during either annealing or passage of current processes, which lead to red-shifted and less-efficient emissions and reduced color purity.[2] Many studies have been carried out to solve the aggregation-related problems by increasing the structural hindrances of PFs and thus to reduce their self-aggregation tendency in the solid state. For example, studies of PFs containing long (or bulky) and branched side chains,[3] copolymerization techniques,[4] dendrimer attachment,[5] end-capping of PFs with bulky groups,[6] cross-linking of PFs,[7] and oligomer approaches[4,8] have been reported.

On the other hand, another problem of PFs is their large band gaps between the LUMO and HOMO energy levels.[9] The high energy barrier between the emissive layer and the electrodes as well as the imbalance between the hole- and electron-transporting properties in the emissive layer are also possible causes of poor performance of a light-emitting diode (LED) device. In this regard, it is well recognized that the charge injection and transport can be facilitated by sandwiching the emissive layer between a hole-injecting/-transporting layer (HTL) above the anode and an electron-injecting/-transporting layer (ETL) under the cathode. An alternative approach addressing these issues is to vary the chemical structures of PFs. For example, the incorporation of electron-withdrawing or electron-donating groups into the PF main chains or side chains can influence the electron- or hole-injecting/-transporting capabilities of the polymers.[10] It is well-known that carbazole-based molecules and polymers are good hole-transporting materials due to the electron-donating capabilities associated with the nitrogen in the carbazole.[11] Several studies of random and alternating fluorene/carbazole copolymers have been designed and synthesized to be used as a light-emitting layer in blue light-emitting diodes.[12] It is demonstrated that the incorporation of 3,6-carbazole units into the fluorene polymer chains will effectively raise the HOMO energy levels and improve the luminescent stability by interfering with the packing order to suppress the aggregation and excimer formation. However, the maxima of UV−vis absorption and PL emission were significantly blue-shifted compared with PF homopolymers, indicating that by copolymerization of PFs with 3,6-linked carbazole units, the effective conjugation lengths of the copolymers have been reduced to some extent. In general, these copolymers showed decreased PL efficiencies compared with PF homopolymers in previous research.

In this study, a series of carbazole/fluorene-based copolymers **(P1−P6)** were prepared by the Suzuki polycondensation reaction, and the influence of the functionalized carbazole units on thermal, photophysical, electrochemical, and electroluminescent properties of the resulting polymers were investigated. The noticeable difference between our investigation and those of previous research is that the properties of polyfluorenes were improved by introducing minimal carbazole derivatives **(2−4)** into poly(2,7−9,9-dihexylfluorene)s to avoid breaking the delocalization of π-electrons seriously along the polymer backbones. To suppress the aggregation phenomena and reduce the excimer formation, "kinked" and "hyperbranched" disordered structures were introduced into the conjugated polyfluorene backbones. Scheme 1 shows the chemical structures and the synthetic procedures of multifunctional carbazole derivatives **(2−4)**. The introduction of hole-transporting dibromocarbazole **(2)** groups into the PF chains can suppress the chain aggregation

* Corresponding author. E-mail: linhc@cc.nctu.edu.tw. Telephone: 8863-5712121 ext. 55305. Fax: 8863-5724727.

10.1021/ma061770j CCC: $33.50
Published on Web 09/21/2006

Scheme 1. Synthetic Routes of Monomers 2−4

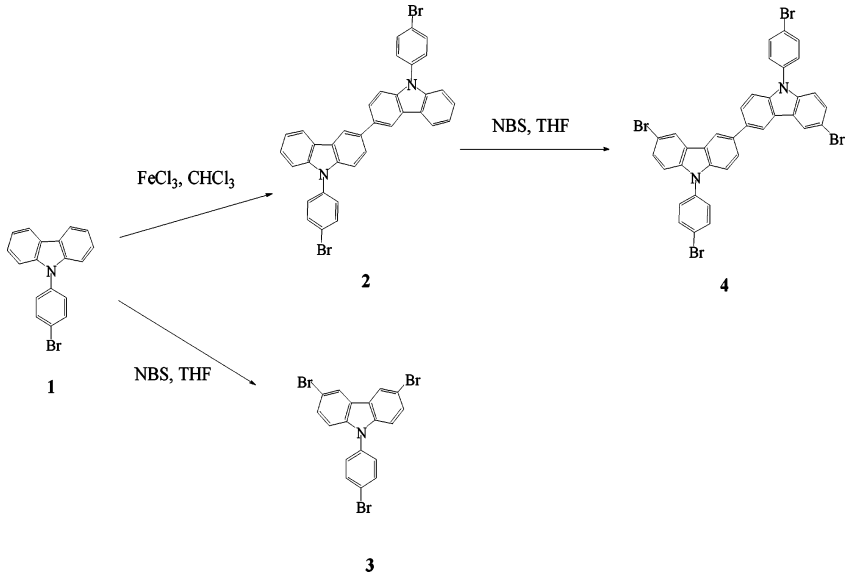

by the formation of kinked linkages and improve the mismatch of energy levels between the anode and PF. In addition, the hyperbranched approach has proven to be an effective method for the design of amorphous nonaggregation in optoelectronic materials.[13,14] It has been well established that the solubility was poor in common organic solvents for hyperbranched polymers with higher contents of branched units by step-growth polymerization. Therefore, a small amount of tribromocarbazole **(3)** or tetrabromocarbazole **(4)** units are suitable as branched units to make the PF polymers with hyperbranched architecture. Thus, PF copolymers with kinked and hyperbranched structures derived from a series of carbazole-based compounds are expected to improve the material properties of polyfluorenes, which can be eventually useful for PLED device applications.

Experimental Section

Materials. Compounds 9-(4-bromophenyl)-9*H*-carbazole **(1)**,[15] 2,7-bis(4,4,5,5-tetramethyl-1,3,2-dioxaborolan-2-yl)-9,9-dihexylfluorene **(5)**,[16] and 2,7-dibromo-9,9-dihexylfluorene **(6)**[16] were synthesized according to the literature procedures. Chemicals and solvents were reagent grade and purchased from Aldrich, ACROS, TCI, and Lancaster Chemical Co. Dichloromethane and THF were distilled to keep anhydrous before use. The other chemicals were used without further purification.

Measurements and Characterization. ^{1}H NMR spectra were recorded on a Varian Unity 300 MHz spectrometer using $CDCl_3$ or 1,4-dioxane solvent. Elemental analyses were performed on a HERAEUS CHN-OS RAPID elemental analyzer. Phase transition temperatures were determined by differential scanning calorimetry (Perkin-Elmer Diamond) with a heating and cooling rate of 10 °C/min. Thermogravimetric analysis (TGA) was conducted on a Du Pont Thermal Analyst 2100 system with a TGA 2950 thermogravimetric analyzer under a heating rate of 20 °C/min. Gel permeation chromatography (GPC) analysis was conducted on a Waters 1515 separation module using polystyrene as a standard and THF as an eluent. UV−visible absorption spectra were recorded in dilute chloroform solutions (10^{-6} M) on a HP G1103A spectrophotometer, and photoluminescence (PL) spectra were obtained on a Hitachi F-4500 spectrophotometer. Thin films of UV−vis and PL measurements were spin-coated on a quartz substrate from chloroform solutions with a concentration of 1 wt %. The relative photoluminescent quantum yields (Φ_{PL}) of the compounds in chloroform were determined using a solution of 9,10-diphenylanthracene as a standard (cyclohexane, $\Phi_{PL} = 0.90$). Dilute sample solutions were used for the determinations (absorbance < 0.1). Values are calculated according to the equation, $\Phi_{unk} = \Phi_{std}(I_{unk}/A_{unk})(A_{std}/I_{std})(\Pi_{unk}/\Pi_{std})^2$, where Φ_{unk} is the fluorescence quantum yield of the sample, Φ_{std} is the fluorescence quantum yield of the standard, I_{unk} and I_{std} are the integrated emission intensities of the sample and the standard, respectively, A_{unk} and A_{std} are the absorbances of the sample and the standard at the excitation wavelength, respectively, and Π_{unk} and Π_{std} are the refractive indexes of the corresponding solutions (pure solvents were assumed). Electrochemistry measurements were performed using an Autolab PGSTAT30 potentiostat/galvanostat with a standard three-electrode electrochemical cell in a 0.1 M tetrabutylammonium hexafluorophosphate ($TBAPF_6$) solution (in acetonitrile) at room temperature with a scanning rate of 100 mV/s. A platinum working electrode, a platinum wire counter electrode, and an Ag/AgCl reference electrode were used. The onset potentials were determined from the intersection of two tangents drawn at the rising current and background current of the cyclic voltammogram (CV).

EL Device Fabrication. The devices were fabricated on ITO substrates that had been ultrasonicated and sequentially washed in detergent, methanol, 2-propanol, and acetone, and further treated with O_3 plasma for 10 min before use. Thin layers of PEDOT (40 nm) on the anode and polymers (from 1 wt % of polymers in chloroform solutions) were consecutively spin-coated on the ITO surface, after which a thin layer of LiF(0.5 nm)/Al(200 nm) was deposited on the polymer films by thermal evaporation under a vacuum of 10^{-6} Torr. All measurements of the EL devices were carried out in air at room temperature. The luminance−current−voltage characteristics were recorded on a power source meter (Keithley 2400) and a photometer (Minolta CS-100A).

Synthesis. The synthetic routes of monomers **2−4** and polymers are shown in Schemes1 and 2, and their synthetic procedures are shown as follows:

9,9′-Bis-(4-bromophenyl)-9*H*,9′*H*-[3,3′]bicarbazolyl (2). To a stirred solution containing 2.93 g (9.1 mmol) of 9-(4-bromophenyl)-9*H*-carbazole **(1)** in 70 mL of chloroform under nitrogen, 3.0 g (18.5 mmol) of iron(III) chloride was added. Water (75 mL) was added after stirring for 40 h at room temperature. The mixture was extracted with CH_2Cl_2, and the organic layer was dried over $MgSO_4$, filtered, and concentrated. The mixture was purified by column chromatography with EA/hexane (1:10) to get a white solid. Yield: 70%. ^{1}H NMR (ppm, $CDCl_3$): δ 7.30−7.39 (m, 4H), 7.41−7.52 (m, 8H), 7.73−7.78 (m, 6H), 8.23 (d, 2H, $J = 7.5$ Hz), 8.43 (d, 2H, $J = 1.2$ Hz). MS (FAB): *m/z* [M^+] 642, calcd *m/z* [M^+] 642.38. Anal. Calcd for $C_{36}H_{22}Br_2N_2$: C 67.31, H 3.45, N 4.36. Found: C 67.28, H 3.68, N 4.42.

3,6-Dibromo-9-(4-bromophenyl)-9*H*-carbazole (3). In a flask covered with aluminum foil, a stirred solution containing 2 g (6.2

Scheme 2. Synthetic Routes of Polymers

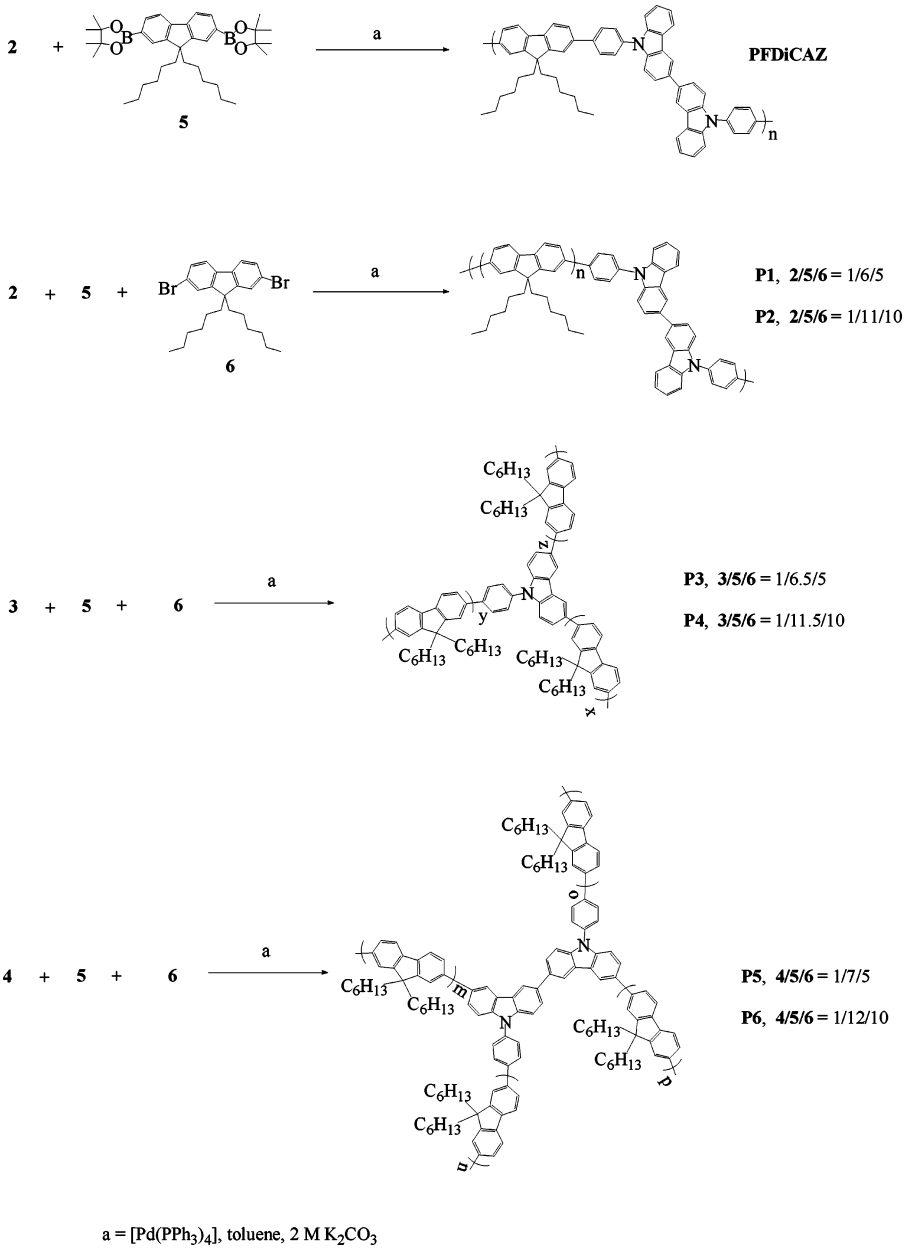

mmol) of 9-(4-bromophenyl)-9*H*-carbazole (**1**) in 200 mL of THF was cooled to 0 °C. *N*-bromosuccinimide (NBS, 2.2 g, 12.4 mmol) was added in small portions. The mixture was allowed to warm to react at room temperature overnight. Then, the solvent was evaporated, and the crude product was purified by extraction with CH_2Cl_2 and water. The combined organic phases were dried over $MgSO_4$. After removal of the solvent, the crude product was further purified by column chromatography on silica gel eluted with CH_2Cl_2/hexane (1:10) and crystallization (acetone), respectively, to afford compound **3** as a white crystal. Yield: 65%. ^{1}H NMR (ppm, $CDCl_3$): δ 7.22 (d, 2H, J = 8.7 Hz), 7.38 (d, 2H, J = 8.4 Hz), 7.51 (dd, 2H, J = 1.5 Hz, J = 8.7 Hz), 7.74 (d, 2H, J = 9.0 Hz), 8.19 (d, 2H, J = 1.8 Hz). MS (EI): m/z [M^+] 480, calcd m/z [M^+] 479.99. Anal. Calcd for $C_{18}H_{10}Br_3N$: C 45.04, H 2.10, N 2.92. Found: C 45.49, H 2.40, N 3.19.

6,6′-Dibromo-9,9′-bis-(4-bromophenyl)-9*H*,9′*H*-[3,3′]bicarbazolyl (4). The synthesis of compound **4** was also followed by the similar procedure of compound **3**. Compound **2** (2 g, 3.1 mmol), 1.1 g (6.2 mmol) of NBS, and 100 mL of THF were used. Compound **4** was purified by column chromatography with CH_2Cl_2/hexane (1:10) to get a white solid. Yield: 73%. ^{1}H NMR (ppm, 1,4-dioxane): δ 7.34 (d, 2H, J = 8.7 Hz), 7.48 (d, 2H, J = 8.4 Hz), 7.55 (dd, 2H, J = 2.1 Hz, J = 8.7 Hz), 7.60 (d, 4H, J = 8.4 Hz), 7.83−7.87 (m, 6H), 8.48 (d, 2H, J = 2.1 Hz), 8.55 (d, 2H, J = 1.2 Hz). MS (FAB): m/z [M^+] 800, calcd m/z [M^+] 800.17. Anal. Calcd for $C_{36}H_{20}Br_4N_2$: C 54.04, H 2.52, N 3.50. Found: C 53.92, H 2.87, N 3.73.

General Procedure for the Synthesis of Polymers. The synthetic route of polymers is shown in Scheme 2. A general procedure of polymerization is proceeded through the Suzuki coupling reaction. The monomers, alq336 and [$Pd(PPh_3)_4$], were dissolved in toluene and 2 M K_2CO_3 (3:2 in volume). The mixture was degassed and stirred at 85 °C for 2 days. After cooling to room temperature, the reaction mixture was poured into 200 mL of methanol. A fibrous solid was obtained by filtration. The obtained solid was followed by the Soxhlet extraction with acetone for 24 h to remove the catalyst residues and oligomers. Because polymers **P3**−**P6** tend to produce insoluble cross-linking portions in the step-growth polymerization, the solid residues of **P3**−**P6** were further extracted with THF using a Soxhlet apparatus for 24 h, and the insoluble solid (cross-linking networks) was discarded. After removal of THF, the soluble polymer products were dried in a vacuum oven for 24 h.

PFDiCAZ. Monomer **2** (219 mg, 0.34 mmol), monomer **5** (200 mg, 0.34 mmol), K_2CO_3 (1.1 g), [$Pd(PPh_3)_4$] (8 mg), toluene (6 mL), and H_2O (4 mL) were used in the reaction mixture. **PFDiCAZ** was obtained as a gray solid. Yield: 85%. ^{1}H NMR (ppm, $CDCl_3$): δ 0.78−0.83 (m, 10H), 1.14 (m, 12H), 2.16 (broad, 4H), 7.37 (t, 2H, J = 6.6 Hz), 7.50 (t, 2H, J = 8.1 Hz), 7.57 (d, 2H, J = 8.4 Hz), 7.64 (d, 2H, J = 8.1 Hz), 7.74 (m, 8H), 7.88 (t, 4H, J = 9.0 Hz), 7.97 (d, 4H, J = 7.8 Hz), 8.30 (d, 2H, J = 7.8 Hz), 8.53 (s, 2H,).

P1. Monomer **2** (27.4 mg, 0.043 mmol), monomer **5** (150 mg, 0.26 mmol), monomer **6** (104.9 mg, 0.21 mmol), K_2CO_3 (1.1 g), [$Pd(PPh_3)_4$] (8 mg), toluene (6 mL), and H_2O (4 mL) were used in the reaction mixture. **P1** was obtained as a light-yellow solid. Yield: 89%. ^{1}H NMR (ppm, $CDCl_3$): δ 0.78 (broad), 1.23 (broad), 2.12 (broad), 7.32−7.35 (broad), 7.47−7.49 (broad), 7.54−7.94 (broad), 8.27 (d, J = 8.1 Hz), 8.50 (s).

P2. Monomer **2** (14.9 mg, 0.023 mmol), monomer **5** (150 mg, 0.26 mmol), monomer **6** (114.5 mg, 0.23 mmol), K_2CO_3 (1.1 g), [$Pd(PPh_3)_4$] (8 mg), toluene (6 mL), and H_2O (4 mL) were used in the reaction mixture. **P2** was obtained as a light-yellow solid. Yield: 80%. ^{1}H NMR (ppm, $CDCl_3$): δ 0.79 (broad), 1.14 (broad), 2.13 (broad), 7.30−7.36 (broad), 7.68 (broad), 7.83 (broad), 8.28 (d), 8.52 (s).

P3. Monomer **3** (18.9 mg, 0.039 mmol), monomer **5** (150 mg, 0.26 mmol), monomer **6** (96.9 mg, 0.20 mmol), K_2CO_3 (3.3 g), [$Pd(PPh_3)_4$] (8 mg), toluene (18 mL), and H_2O (12 mL) were used in the reaction mixture. **P3** was obtained as a light-yellow solid. Yield: 62%. ^{1}H NMR (ppm, $CDCl_3$): δ 0.78 (broad), 1.12 (broad), 2.09 (broad), 7.22−7.28 (broad), 7.67 (broad), 7.82 (broad), 8.39 (s), 8.54 (s).

P4. Monomer **3** (10.7 mg, 0.022 mmol), monomer **5** (150 mg, 0.26 mmol), monomer **6** (109.5 mg, 0.22 mmol), K_2CO_3 (3.3 g), [$Pd(PPh_3)_4$] (8 mg), toluene (18 mL), and H_2O (12 mL) were used in the reaction mixture. **P4** was obtained as a light-yellow solid. Yield: 74%. ^{1}H NMR (ppm, $CDCl_3$): δ 0.78 (broad), 1.13 (broad), 2.11 (broad), 7.27−7.30 (broad), 7.57 (broad), 7.82−7.85 (broad), 8.45 (s), 8.56 (s).

P5. Monomer **4** (29.2 mg, 0.037 mmol), monomer **5** (150 mg, 0.26 mmol), monomer **6** (90 mg, 0.18 mmol), K_2CO_3 (3.3 g), [$Pd(PPh_3)_4$] (8 mg), toluene (18 mL), and H_2O (12 mL) were used in the reaction mixture. **P5** was obtained as a light-yellow solid. Yield: 43%. ^{1}H NMR (ppm, $CDCl_3$): δ 0.80 (broad), 1.22 (broad), 2.12 (broad), 7.26−7.36 (broad), 7.51−7.58 (broad), 7.68 (broad), 7.83−7.86 (broad), 8.59 (broad).

P6. Monomer **4** (17.1 mg, 0.021 mmol), monomer **5** (150 mg, 0.26 mmol), monomer **6** (104.9 mg, 0.21 mmol), K_2CO_3 (3.3 g), [$Pd(PPh_3)_4$] (8 mg), toluene (18 mL), and H_2O (12 mL) were used in the reaction mixture. **P6** was obtained as a light-yellow solid. Yield: 55%. ^{1}H NMR (ppm, $CDCl_3$): δ 0.79 (broad), 1.21 (broad), 2.11 (broad), 7.30 (broad), 7.35 (broad), 7.67 (broad), 7.82 (broad), 8.58 (broad).

Results and Discussion

Synthesis and Characterization. Scheme 1 shows the synthetic routes of monomers **2**−**4**. 9-(4-Bromophenyl)-9*H*-carbazole (**1**) was synthesized from carbazole as the starting material by a modified Ullmann reaction.[15b] Two of compound **1** were linked via the 3- or 6-position of carbazoles to form dibromocarbazole monomer **2**. NBS was used to brominate compound **1** or **2** to produce tribromocarbazole monomer **3** or tetrabromocarbazole monomer **4**, respectively, with high yields. Monomers **2**−**4** were satisfactorily characterized by ^{1}H NMR, MS spectroscopy, and elemental analyses. The synthetic routes of **PFDiCAZ** and **P1**−**P6** are shown in Scheme 2. **PFDiCAZ**, **P1**, and **P2** were obtained by reaction of **2**, **5**, and **6** with different molar ratios in toluene containing $Pd(PPh_3)_4$ (1 mol %). The obtained polymers were further purified by washing with acetone in a Soxhlet apparatus for 24 h to remove oligomers and catalyst residues and were dried under reduced pressure at room temperature. After purification and drying, **PFDiCAZ**, **P1**, and **P2** were obtained as yellow fibrous solids in overall good yields. **P3** and **P4** were synthesized by reacting monomers **3**, **5**, and **6** with different molar ratios. The molar ratios of monomer **3** in copolymers were found to be key factors of the solubilities in hyperbranched **P3** and **P4**. The solubilities were poor in common organic solvents for hyperbranched polymers with higher contents of monomer **3**. The polymers with the molar ratios (monomer **3/5/6**) of 1:6.5:5 (**P3**) and 1:11.5:10 (**P4**) were approximately soluble in THF. **P3** and **P4** were purified by two-step extractions: first with acetone to remove catalyst residues and unreacted monomers (soluble in acetone), and then with THF to extract the soluble portions of hyperbranched polymers (insoluble cross-linking parts were discarded). The synthesis of **P5** and **P6** were also followed according to the synthetic procedures of **P3** and **P4** by reacting monomers **4**, **5**, and **6** with different molar ratios. The obtained **PFDiCAZ** and **P1**−**P6** exhibited good solubilities in common organic solvents, e.g., toluene, THF, and chloroform.

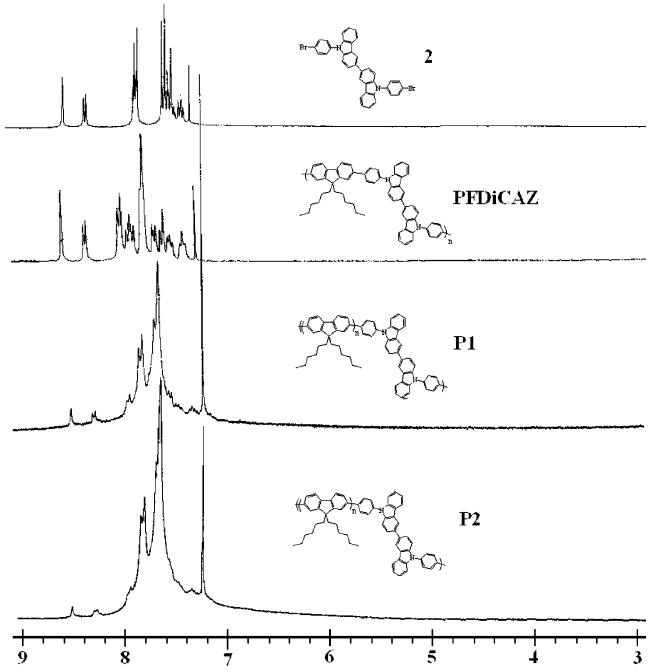

Figure 1. ^{1}H NMR spectra of monomer **2**, **PFDiCAZ**, **P1**, and **P2**.

Figure 1 shows ^{1}H NMR spectra of monomer **2**, **PFDiCAZ**, **P1**, and **P2** in $CDCl_3$. ^{1}H NMR spectra of **PFDiCAZ**, **P1**, and **P2** showed doublet signals at δ = 8.3 and singlet signals at δ = 8.5, respectively, which were assigned to the proton signals of 9,9′-diphenyl-bicarbazolyl linkages. Comparing ^{1}H NMR spectra of **PFDiCAZ**, **P1**, and **P2**, it was found that the integrated signals of the kinked units increased with more amounts of monomer **2** added. The number-average molecular weights and the weight-average molecular weights of the polymers listed in Table 1 were 15100−24300, and 34500−66300, respectively, which were determined by means of gel permeation chromatography (GPC) using THF as eluent against polystyrene standards.

Thermal Properties. The thermal stability of the polymers was determined by thermogravimetric analysis (TGA) under nitrogen. As shown in Table 1, all of these polymers possess excellent thermal stability with 5% weight loss temperatures (T_ds) ranging from 407 to 466 °C. These data reveal that all polymers have excellent thermal stability.

Thermally induced phase transition properties of the polymers were also investigated by differential scanning calorimetry

Table 1. Molecular Weights and Thermal Properties of Polymers

polymer	M_n[a]	M_w[a]	PDI	T_g (°C)[b]	T_d (°C)[c]
PFDiCAZ	23400	43600	1.87	n.d.[d]	466
P1	24300	39900	1.64	109	424
P2	21400	40600	1.90	115	420
P3	15100	34500	2.28	140	433
P4	21800	66300	3.04	120	449
P5	15500	49500	3.19	n.d.[d]	407
P6	17800	49500	2.78	n.d.[d]	407

[a] Molecular weight determined by GPC in THF, based on polystyrene standards. [b] Glass transition temperature (°C) determined by DSC at a heating rate of 10 °C min^{-1} under nitrogen. [c] Temperature (°C) at 5% weight loss measured by TGA at a heating rate of 20 °C min^{-1} under nitrogen. [d] No noticeable T_g was observed.

Table 2. Absorption and PL Emission Spectral Data of Polymers in Solution and Solid States

polymer	$\lambda_{Abs,sol}$ (nm)[a]	$\lambda_{PL,sol}$ (nm)[a]	$\lambda_{Abs,film}$ (nm)	$\lambda_{PL,film}$ (nm)	band gap (eV)[b]	$\Phi_{PL,sol}$[c]	$\Phi_{PL,rel}$[d]
PFDiCAZ	351	402	355	414	3.1	0.47	0.44
P1	380	417, 440	379	425, 444	2.9	0.99	0.94
P2	388	417, 440	380	424, 447	2.9	0.94	0.88
P3	380	417, 440	388	423, 445	2.9	0.96	0.90
P4	388	417, 440	380	424, 444	2.9	0.81	0.76
P5	380	417, 441	388	422, 446	2.9	0.90	0.85
P6	388	417, 440	388	423, 446	2.9	0.88	0.83

[a] Chloroform as solvent with a concentration of 10^{-6} M. [b] Band gaps were calculated from the onsets of UV−visible absorption spectra of **P1**−**P3** in solid films. [c] Solution fluorescence quantum efficiency measured in chloroform, relative to 9,10-diphenylanthracene in cyclohexane ($\Phi_{PL} = 0.9$). [d] Relative fluorescence quantum efficiencies in solutions were estimated relative to the synthesized PF homopolymer, i.e., poly-2,7-(9,9-dihexylfluorene) as a reference, with $M_n = 26700$, PDI = 1.94, and $\Phi_{PL,rel} = 1$.

(DSC) under nitrogen. PF homopolymer had a crystallization temperature of 113 °C and a melting point of 159 °C, indicating the crystalline nature of this polymer as reported previously.[17] The incorporation of a series of carbazole units into the copolymers resulted in DSC traces that show no crystallization and melting peaks but only glass transition temperatures (T_gs). This clearly indicates that the presence of the kinked or hyperbranched structures in these copolymers effectively suppresses the crystallizability (or chain aggregation) of the polymer chains. The glass transition temperatures (T_gs) of **P1**−**P4** were ranged from 109 to 140 °C. Compared with **P2** possessing analogous kinked molecular architectures, **P1** with a higher kinked carbazole content has lower T_g, which is conceivable by reason of a higher kinked density of carbazole units in **P1**. Compared with **P4** possessing similar hyperbranched molecular architectures, **P3** with a higher hyperbranched carbazole content has higher T_g, which is plausible because of a higher hyperbranched density of carbazole units in **P3**. Hence, polymers with higher kinked density or lower hyperbranched density of carbazole units possess lower T_g relatively. No distinct glass transitions were observed for **PFDiCAZ**, **P5**, and **P6** in their DSC curves of the second heating. In addition, the measured values of T_ds and T_gs were higher than that of the linear polyfluorene.[18]

Optical Properties. UV−vis absorption and PL emission data of the polymers are shown in Table 2 and Figures2−5. **PFDiCAZ** (alternative copolymers) displayed an absorption maximum ($\lambda_{Abs,sol}$) at 351 nm in $CHCl_3$ solution, resulting in a substantially blue shift compared with that of PF homopolymer. This behavior is similar to the analogous alternating fluorene/carbazole copolymers,[19] which is due to the interruption of the delocalization of π-electrons along the polymer backbones by 9,9′-diphenyl-bicarbazolyl linkages. This effect also manifests

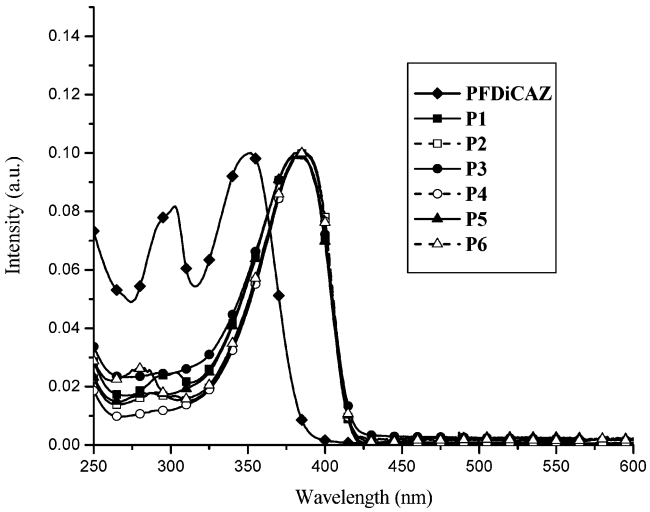

Figure 2. Normalized UV−vis absorption spectra of polymers in chloroform (10^{-6} M).

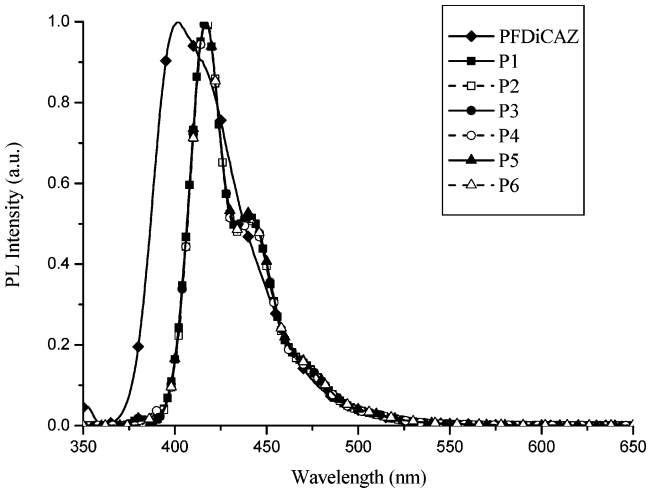

Figure 3. Normalized PL spectra of polymers excited at the maximum absorption of the polymer backbones in chloroform (10^{-6} M).

itself in the solution PL spectrum, where the emission peak is blue-shifted to 402 nm as compared with that of PF. With considerable decreases in the amounts of 9,9′-diphenyl-bicarbazolyl moieties, **P1** and **P2** show their absorption peaks with the values of $\lambda_{Abs,sol} = 380$ nm for **P1** and $\lambda_{Abs,sol} = 388$ nm for **P2** (which are close to those of PF). In the case of hyperbranched polymers, the absorption peaks in solutions appeared at 380 nm for **P3** and **P5**, and 388 nm for **P4** and **P6**, were similar to those of copolymers **P1** and **P2**. The result indicated that the absorption maxima are blue-shifted in analogous systems with the increasing contents of kinked or branching units. Compared with the absorption spectra of monodisperse oligofluorenes reported in the literature,[20] the average conjugated lengths of the polymers can be estimated. According to this assumption, **P1**, **P3**, and **P5** should have comparable persistent conjugation lengths to that of an oligomer with eight fluorene units. However, the average conjugated lengths of **P2**, **P4**, and **P6** are not conceivable but similar to those of PF homopolymers with high molecular weights. It has been reported that, as the number of fluorene units is larger than five, the emission wavelengths of the oligofluorenes approach those of polyfluorenes with high molecular weights.[20] As shown in Figure 3, the PL spectra of **P1**−**P6** in $CHCl_3$ solutions are strikingly similar to each other, which show the maximum band around 417 nm along with a vibronic band at 440 nm. In general, the

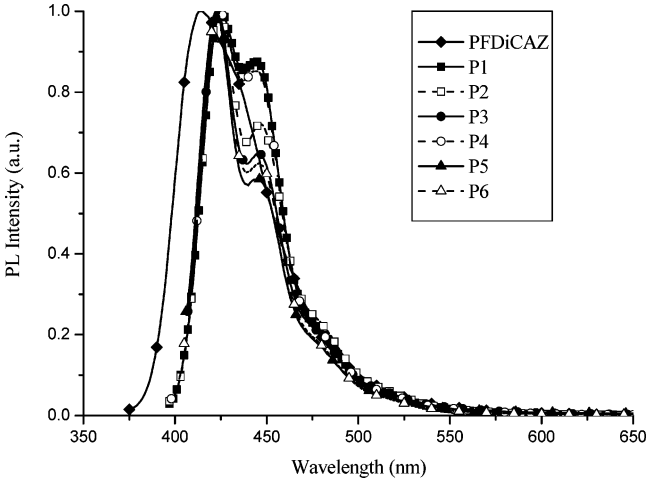

Figure 4. Normalized PL spectra of polymers excited at the maximum absorption of the polymer backbones in solid films.

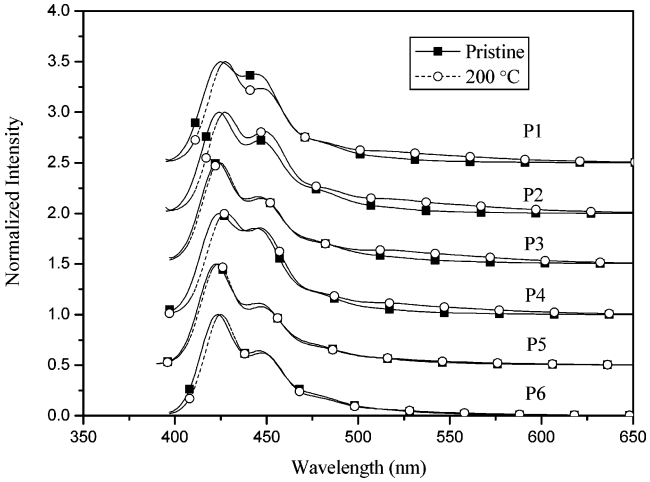

Figure 5. Normalized PL spectra of polymers excited at the maximum absorption of the polymer backbones in solid films: before annealing (pristine film) and annealing at 200 °C for 0.5 h under air.

presence of well-defined vibronic structures in the emission spectra indicates that the polymers have rigid and well-defined backbone structures.[21] The similar emissions observed for these copolymers in comparison with that of PF homopolymer might suggest that the carbazole derivatives in the polymer backbones do not prevent efficient energy transfer from the short conjugated emissions to the long ones in these copolymers. Therefore, as discussed above, the carbazole segments of the copolymers efficiently interrupt the conjugation of the polymer backbones, but most of the excitons migrate to the fluorene segments to emit light with lower energy. UV−vis and PL spectra of thin solid films were measured by spin-coating of solutions on quartz substrates. The optical band gaps (E_g) of **P1**−**P6** were determined to be around 2.9 eV from the UV−vis absorption spectra (solid films). As shown in Figure 4, the PL spectra of all polymers in the solid state showed 5−8 nm of red-shifts and some broadening of the emission bands in comparison with their solution PL spectra. Unlike the PL spectrum of polyfluorene possessing an aggregation peak around 520 nm besides two excitonic emission peaks, the PL spectra of **P1**−**P6** only show peaks at 424 and 446 nm. The lack of the excimer emission in the solid films of **P1**−**P6** proves that even introducing a small amount of carbazole derivatives can influence the packing of the polymer chains in the solid state and thus to enhance the quantum efficiency.

To investigate luminescent stability of the polymers in the solid state, annealing experiments were performed on polymers **P1**−**P6**. Because the incorporation of the carbazole derivatives into PFs in this work suppressed the crystallizability of the polymers by lack of crystallization and melting peaks in the DSC measurements, it could be expected that these copolymers would be prone to have less chain aggregation and thus to possess improved fluorescent stabilities. After being spin-coated on a quartz substrate, the solid film was annealed at 200 °C for 1 h under nitrogen. Annealing at such a temperature, which is much higher than the glass transition temperature, can cause the movement of chain segments and increase the packing order. In fact, annealing of **PFDiCAZ** and **P1**−**P6** at 200 °C for 1 h under nitrogen resulted in no obvious changes in the PL spectra as compared with those of pristine (as-prepared) films. There was no additional band that emerged to change the pure-blue emission into another undesirable blue-green color. This clearly suggests that the formation of excimer aggregation in these copolymers is effectively suppressed even at temperatures much higher than their T_gs. However, different results can be observed after annealing at 200 °C under air because traces of defects formed via oxidation could also cause drastic spectral changes.[22] As shown in Figure 5, PL spectra of kinked polymers **P1** and **P2** show a little change at the peak of 445 nm by annealing at 200 °C for 0.5 h under air. In comparison with kinked polymers **P1** and **P2**, all hyperbranched polymers **P3**−**P6** have better thermal stability by annealing under air (but no difference under nitrogen). Besides, PL spectra of **P1**−**P4** showed a weak long wavelength emission tail around 520 nm after annealing under air. These changed features of PL spectra were attributed to the interchain excimer formation and/or keto defects, which are commonly observed in 9,9-disubstituted PFs after annealing.[23] Nevertheless, the excimer peak increases very slowly compared with previously reported PF homopolymers.[24] It is noteworthy that no green-blue band emission was observed in the thermal treatment of **P5** and **P6**. Apparently, the introduction of kinked or hyperbranched disorder in the conjugated polymer chains shows more stable PL spectra of these copolymers upon annealing, where the aggregation and excimer formation of polymer chains can be avoided efficiently. Similar phenomenon regarding the effect of disorder on chromic behavior for other polyfluorene copolymers have also been reported by Leclerc,[25] which was attributed to the increased conformational flexibility of the copolymers to interchain interaction, resulting in the incorporation of nonfluorene comonomer units. The PL quantum yields (Φ_{PL}) of **PFDiCAZ** and **P1**−**P6** excited at the maximum absorption of the polymer backbones in solutions were measured with 9,10-diphenylanthracene as a reference standard (cyclohexane, $\Phi_{PL} = 0.90$).[26] Except **PFDiCAZ**, the quantum efficiencies of **P1**−**P6** reach 0.81−0.99, which are much higher than the hyperbranched polyfluorene in the previous report.[27] The high PL quantum yields (Φ_{PL}) of these polymers were attributed to the introduction of minimal carbazole derivatives into poly(2,7-9,9-dihexylfluorene) to avoid reducing the effective conjugation lengths of the copolymers seriously. Besides, The PL quantum yields (Φ_{PL}) of polymers **P1**−**P6** were also compared with that of PF homopolymer, i.e., poly-2,7-(9,9-dihexylfluorene). The values of Φ_{PL} for **P1**−**P6** are slightly lower than that of PF homopolymer. The measured data of PL quantum yields are listed in Table 2.

Electrochemical Characterization. The electrochemical properties of the polymers were investigated by using cyclic voltammetry (CV), and their anodically scanned cyclic voltammograms are shown in Figure 6. **PFDiCAZ** (50% of the fluorene units was replaced by diphenylcarbazole units) exhibited reversible processes in the oxidation scan and had an

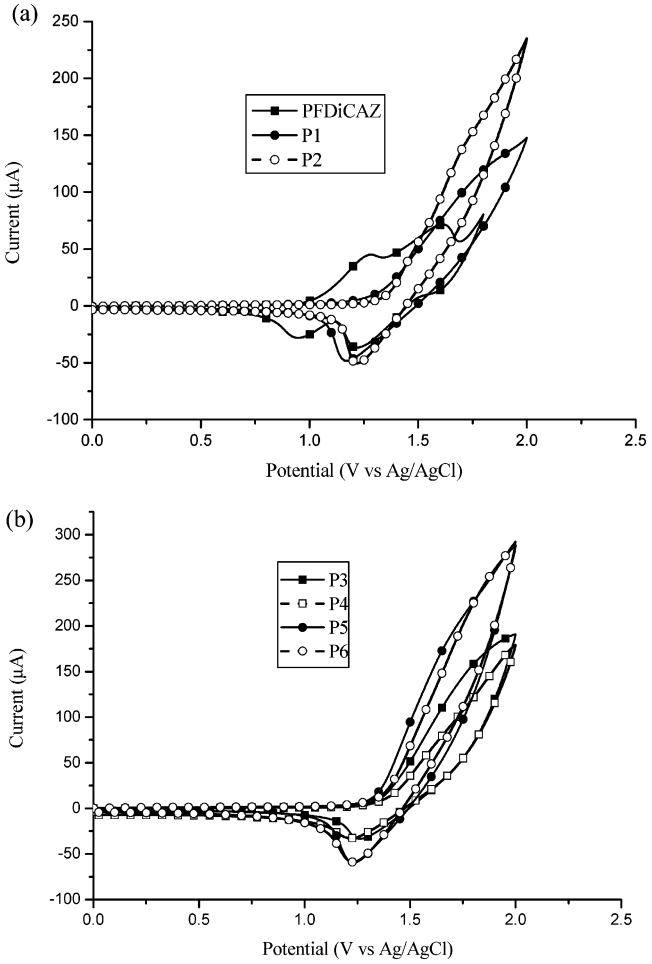

Figure 6. Cyclic voltammograms of the polymers: (a) **PFDiCAZ**, **P1**, and **P2**; (b) **P3**, **P4**, **P5**, and **P6**.

oxidative onset potential at 0.96 V that was much lower than the reported value (1.4 V) of poly(9,9-dioctylfluorene) (POF).[28] The decrease of the oxidative onset potential indicated the introduction of the 9,9′-diphenyl-bicarbazolyl linkages facilitates better hole injection from the ITO anode. When the 9,9′-diphenyl-bicarbazolyl contents decreased substantially, the co-polymers display a slightly higher onset potential of oxidation with values of 1.20 V for **P1** and 1.28 V for **P2**, but still lower than the value of POF. The similar effect was also observed in the previous report where only a small amount of carbazole units was incorporated into the polymers.[19] It is noticeable that the onset potential of oxidation in **P1** is slightly lower than that in **P2** due to the higher carbazole content in **P1**. In the meanwhile, similar trends were also observed in the oxidation processes of hyperbranched polymers **P3**-**P6**. The HOMO energy values of the polymers were estimated according to that (−4.8 eV) of ferrocene (Fc) with respect to zero vacuum level. Furthermore, the optical absorption edge was utilized to derive the band gap and calculate the LUMO energy values for the polymers.[29] The measured oxidation potentials along with HOMO and LUMO energy values of the polymers are summarized in Table 3. As a result, all of the polymers have higher HOMO energy levels than that of the POF, which means that better hole-transporting capabilities can be expected in polymers **P1**−**P6**.

Electroluminescence (EL) Properties. Owing to the short conjugation length and low PL efficiency of **PFDiCAZ**, the applications of polymers **P1**, **P3**, and **P5** in PLED devices were surveyed in this study. The representative polymers **P1**, **P3**, and **P5** were used as emitting layers in double-layered PLED devices

Table 3. Oxidation Potentials and HOMO and LUMO Energy Values of Polymers

polymer	$E_{ox/onset}$ (V)	HOMO (eV)	LUMO (eV)[a]
PFDiCAZ	0.96	−5.36	−2.26
P1	1.20	−5.60	−2.70
P2	1.32	−5.72	−2.82
P3	1.33	−5.73	−2.83
P4	1.36	−5.76	−2.86
P5	1.27	−5.67	−2.77
P6	1.36	−5.76	−2.86

[a] LUMO energy values were deduced from HOMO energy values and optical band gaps.

Table 4. EL Data of PLED Devices[a]

polymer	λ_{EL} (nm)	fwhm (nm)	V_{on}[b] (V)	power efficiency (cd/A)[c]	luminance efficiency (cd/W)[c]	max brightness (cd/m^2)
P1	425	42	7	0.11	0.05	133 (14 V)
P3	426	42	6	0.35	0.08	213 (13 V)
P5	421	39	8	0.07	0.03	87 (13 V)

[a] Device structure: ITO/PEDOT/Polymer/LiF/Al. [b] V_{on}: the turn-on voltage of light. [c] Measured at 100 mA/cm^2.

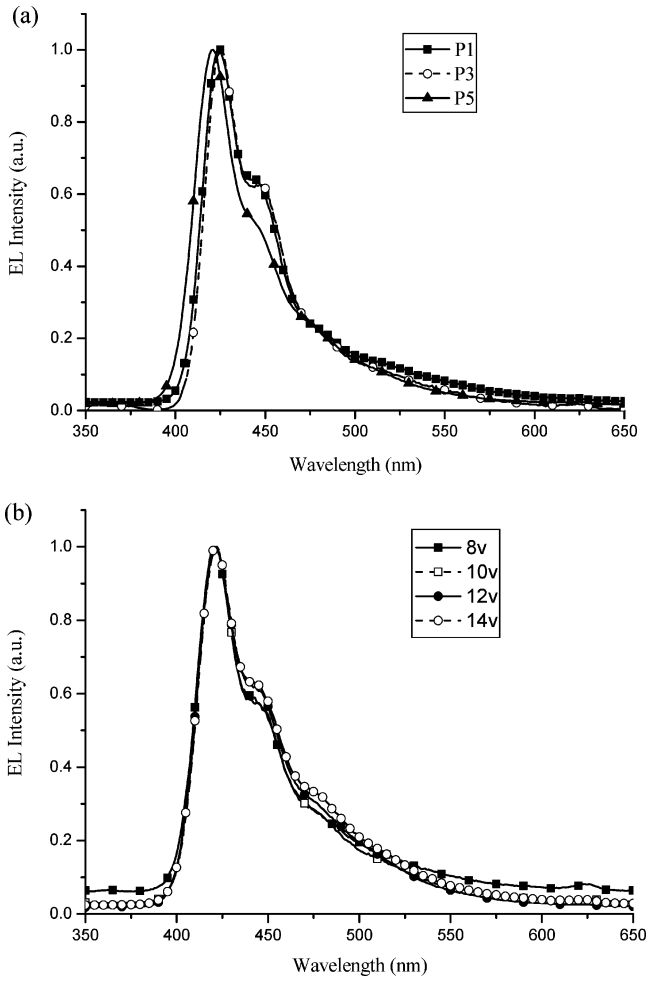

Figure 7. (a) Normalized EL spectra of **P1**, **P3**, and **P5** at 10 V. (b) Normalized EL spectra of ITO/PEDOT/**P3**/LiF/Al device at different voltages.

with a configuration of ITO/PEDOT:PSS/polymer/LiF/Al, and their EL data of PLED devices are shown in Table 4. As can be seen in Figure 7(a), the pure-blue EL emissions with negligible emissions in the region of 500−600 nm (which commonly appears for PF-based PLEDs) can be achieved from **P1**, **P3**, and **P5**. In Figure 7b, the EL spectra of **P3** are almost unchanged and without any low-energy emission bands as the

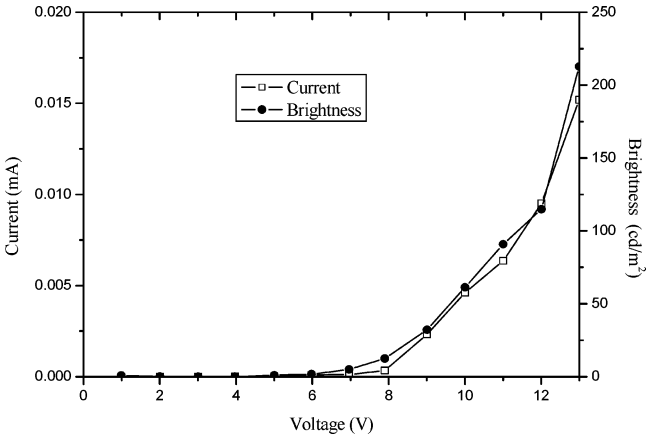

Figure 8. Current−voltage−brightness (*I-V-B*) characteristics of the PLED device containing **P3** with the configuration of ITO/PEDOT/**P3**/LiF/Al.

voltage was increased from 8 to 14 V. The fwhm values of the EL spectra in **P1**, **P3**, and **P5** are 42, 42, and 39 nm, respectively. The narrow EL spectra of these polymers are almost identical to the PL spectra of the corresponding polymer films. Figure 8 shows the current and luminance of PLED device containing **P3** as a function of the applied voltage. The device emitted bright-blue light starting at about 6.0 V and reached a brightness of 213 cd/m^2 at a bias voltage of 13 V. The results suggest that the improvement in EL device performance with these copolymers is due to the introduction of kinked or hyperbranched disorder in the conjugated polymer chains. These preliminary data show the applicability of these novel polymers as PLED blue-emitters.

Conclusion

In summary, a series of novel kinked and hyperbranched carbazole/fluorene-based copolymers by one-pot Suzuki polycondensation (SPC) were successfully synthesized. The polymers exhibited high thermal stability with their decomposition temperatures (T_ds) in the range of 407−466 °C. The PL quantum efficiencies of **P1**−**P6** in chloroform solutions were in the range of 0.81−0.99. The PL spectra of **P1**−**P6** in solid films exhibited similar spectral patterns (only with 5−8 nm of red-shift in their emission maxima) in contrast to those measured in solutions. No long wavelength excimer-like emissions at 500−600 nm attributed to self-aggregation of polyfluorenes in the solid state were observed in these polymers. Thus, the polymers were less easy to self-aggregate in the solid state due to their kinked and hyperbranched structures. The polymer films exhibited very stable blue light emission even annealing at 200 °C for 1 h under nitrogen. Besides, the tunability of hole-transporting properties and the stability of excellent luminescent properties were all demonstrated by these kinked and hyperbranched structures, which render them promising candidates for use as light-emitting materials in stable blue PLED devices. Thus, the possibility of improved luminescence properties in polyfluorene materials through carbazole copolymerization has been demonstrated.

Acknowledgment. We thank the financial support from the National Science Council of Taiwan (ROC) through NSC 93-2113-M-009-011. Prof. Kung-Hwa Wei (CV and GPC measurements) at the Department of Materials Science and Engineering, National Chiao Tung University (in Taiwan), and Mr. Menq-Dan Jiang (vacuum deposition systems) at the Chung-Shan Institute of Science and Technology (in Taiwan) are also acknowledged for their instrumental support.

References and Notes

(1) (a) Pei, Q.; Yang, Y. *J. Am. Chem. Soc.* **1996**, *118*, 7416. (b) Leclerc, M. *J. Polym. Sci., Part A: Polym. Chem.* **2001**, *22*, 1365. (c) Grice, A. W.; Bradeley, D. D. C.; Bernius, M. T.; Inbasekaran, M.; Wu, W. W.; Woo, E. P. *Appl. Phys. Lett.* **1998**, *73*, 629.

(2) (a) Craig, M. R.; de Kok, M. M.; Hofstraat, J. W.; Schenning, A. P. H. J.; Meijer, E. W. *J. Mater. Chem.* **2003**, *13*, 2861. (b) Jenekhe, S. A.; Osaheni, J. A. *Science* **1994**, *265*, 765. (c) Gong, X.; Iyer, P. K.; Moses, D.; Bazan, G. C.; Heeger, A. J.; Xiao, S. S. *Adv. Funct. Mater.* **2003**, *13*, 325.

(3) (a) List, E. J. W.; Güntner, R.; Scandiucci de Freitas, P.; Scherf, U. *Adv. Mater.* **2002**, *14*, 374. (b) Grell, M.; Knoll, W.; Lupo, D.; Meisel, A.; Miteva, T.; Neher, D.; Nothofer, H. G.; Scherf, U.; Yasuda, A. *Adv. Mater.* **1999**, *11*, 671. (c) List, E. J. W.; Partee, J.; Shinar, J.; Scherf, U.; Müllen, K.; Graupner, W.; Petritsch, K.; Zojer, E.; Leising, G. *Phys. Rev. B* **2000**, *61*, 10807. (d) Sung, H. H.; Lin, H. C. *J. Polym. Sci., Part A: Polym. Chem.* **2005**, *43*, 2700.

(4) (a) Pschirer, N. G.; Bunz, U. H. F. *Macromolecules* **2000**, *33*, 3961. (b) Schmitt, C.; Nothofer, H. G.; Falcou, A.; Scerf, U. *Macromol. Rapid Commun.* **2001**, *22*, 624. (c) Kreyenschmidt, M.; Klaerner, G.; Fuhrer, T.; Ashenhurst, J.; Karg, S.; Chen, W. D.; Lee, V. Y.; Scott, J. C.; Miller, R. D. *Macromolecules* **1998**, *31*, 1099. (d) Lee, J. I. G.; Daver, M. H.; Miller, R. D. *Synth. Met.* **1999**, *102*, 1087. (e) Liu, B.; Yu. W. L.; Lai, Y. H.; Huang, W. *Macromolecules* **2000**, *33*, 8945. (f) Sung, H. H.; Lin, H. C. *Macromolecules* **2004**, *37*, 7945.

(5) (a) Setayesh, S.; Grimsdale, A. C.; Weil, T.; Enkelmann, V.; Müllen, K.; Meghdadi, F.; List, E. J. W.; Leising, G. *J. Am. Chem. Soc.* **2001**, *123*, 946. (b) Marsitzky, D.; Vestberg, R.; Blainey, P.; Tang, B. T.; Hawker, C. J.; Carter, K. R. *J. Am. Chem. Soc.* **2001**, *123*, 6965. (c) Klärner, G.; Miller, R. D.; Hawker, C. J. *Polym. Prepr. (Am. Chem. Soc., Div. Polym. Chem.)* **1998**, *39*, 1006. (d) Berresheim, A. J.; Müller, M.; Müllen, K. *Chem. Rev.* **1999**, *99*, 1747. (e) Morgenroth, F.; Reuter, E.; Müllen, K. *Angew. Chem.* **1997**, *109*, 647; *Angew. Chem., Int. Ed. Engl.* **1997**, *36*, 631. (f) Chou, C. H.; Shu, C. F. *Macromolecules* **2002**, *35*, 9673. (g) Fu, Y.; Li, Y.; Li, J.; Yan, S.; Bo, Z. *Macromolecules* **2004**, *37*, 6395. (h) Wu, C. W.; Tsai, C. M.; Lin, H. C. *Macromolecules* **2006**, *39*, 4298. (i) Wu, C. W.; Sung, H. H.; Lin, H. C. *J. Polymer Sci., Part A: Polymer Chem.* **2006**, in press.

(6) (a) Klärner, G.; Miller, R. D.; Hawker, C. J. *Polym. Prepr. (Am. Chem. Soc., Div. Polym. Chem.)* **1998**, 1047. (b) Miteva, T.; Meisel, A.; Knoll, W.; Nothofer, H. G.; Scherf, U.; Müller, D. C.; Meerholz, K.; Yasuda, A.; Neher, D. *Adv. Mater.* **2001**, *13*, 565. (c) Lee, J. L.; Hwang, D. *Synth. Met.* **2000**, *111*, 195.

(7) (a) Klaener, G.; Lee, J. L.; Lee, V. Y.; Chan, E.; Chen, J. P.; Nelson, A.; Markiewicz, D.; Siemens, R.; Scott, J. C.; Miller, R. D. *Chem. Mater.* **1999**, *11*, 1800. (b) Chen, J. P.; Klaerner, G.; Lee, J. I.; Mrkiewicz, D.; Lee, V. Y.; Miller, R. D.; Scott, J. C. *Synth. Met.* **1999**, *107*, 129. (c) Cho, H. J.; Jung, B. J.; Cho, N. S.; Lee, J.; Shim, H. K. *Macromolecules* **2003**, *36*, 6704.

(8) (a) *Electronic Materials: The Oligomer Approach*; Müllen, K., Wegner, G., Eds.; Wiley-VCH: Weinheim, **1998**. (b) Geng, Y.; Trajkovska, A.; Katsis, D.; Ou, J. J.; Culligan, S. W.; Chen, S. H. *J. Am. Chem. Soc.* **2002**, *124*, 8337. (c) Porzio, W.; Botta, C.; Destri, S.; Pasini, M. *Synth. Met.* **2001**, *122*, 7. (d) Lee, S. H.; Tsutsui, T. *Thin Solid Films* **2000**, *363*, 76. (e) Jo, J.; Höger, S.; Wegner, G.; Yoon, D. Y. *Polym. Prepr. (Am. Chem. Soc., Div. Polym. Chem.)* **2002**, *43*, 1118

(9) Wu, W.; Bernius, M.; Dibbs, M.; Inbasekaran, M.; Woo, E.; Wujkowski, L. *Polym. Prepr. (Am. Chem. Soc., Div. Polym. Chem.)* **2000**, *41*, 821.

(10) (a) Liu, M. S.; Jiang, X.; Herguth, P.; Jen, A. K. Y. *Chem. Mater.* **2001**, *13*, 3820. (b) Kim, J. L.; Kim, J. K.; Cho, H. N.; Kim, D. Y.; Kim, C. Y.; Hong, S. *Macromolecules* **2000**, *33*, 5880. (c) Liu, S.; Jiang, X.; Ma, H.; Liu, M. S.; Jen, A. K. Y. *Macromolecules* **2000**, *33*, 3514. (d) Shu, C. F.; Dodda, R.; Wu, F. I.; Liu, M. S.; Jen, A. K. Y. *Macromolecules* **2003**, *36*, 6698. (e) Wu, F. I.; Reddy, D. S.; Shu, C. F.; Liu, M. S.; Jen, A. K. Y. *Chem. Mater.* **2003**, *15*, 269.

(11) Stephan, O.; Vial, J. C. *Synth. Met.* **1999**, *106*, 115.

(12) (a) Li, Y.; Ding, J.; Day, M.; Tao, Y.; Lu, J.; D'iorio, M. *Chem. Mater.* **2004**, *16*, 2165. (b) Du, J.; Fang, Q.; Bu, D.; Ren, S.; Cao, A.; Chen, X. *Macromol. Rapid Commun.* **2005**, *26*, 1651.

(13) Xin, Y.; Wen, G. A.; Zeng, W. J.; Zhao, L.; Zhu, X. R.; Fan, Q. L.; Feng, J. C.; Wang, L. H.; Wei, W.; Peng, B.; Cao, Y.; Huang, W. *Macromolecules* **2005**, *38*, 6755.

(14) (a) Liu, X. M.; Lin, T.; Huang, J.; Hao, X. T.; Ong, K. S.; He, C. *Macromolecules* **2005**, *38*, 4157. (b) Liu, X. M.; Xu, J.; Lu, X.; He, C. *Macromolecules* **2006**, *39*, 1397. (c) Liu, X. M.; He, C.; Hao, X. T.; Tan, L. W.; Li, Y.; Ong, K. S. *Macromolecules* **2004**, *37*, 5965. (d) Liu, X. M.; He, C.; Huang, J.; Xu, J. *Chem. Mater.* **2005**, *17*, 434.

(15) (a) Koene, B. E.; Loy, D. E.; Thompson, M. E. *Chem. Mater.* **1998**, *10*, 2235. (b) Gauthier, S.; Fréchet, J. M. J. *Synthesis* **1987**, 383.

(16) Ranger, M.; Rondeau, D.; Leclerc, M. *Macromolecules* **1997**, *30*, 7686.
(17) Grell, M.; Bradley, D. D. C.; Inbasekaran, M.; Woo, E. P. *Adv. Mater.* **1997**, *9*, 798.
(18) Liu, B.; Yu, W.; Lai, Y.; Huang, W. *Chem. Mater.* **2001**, *13*, 1984.
(19) Xia, C.; Advincula, R. C. *Macromolecules* **2001**, *34*, 5854.
(20) Klaerner, G.; Miller, R. D. *Macromolecules* **1998**, *31*, 2007.
(21) (a) Braun, D.; Heeger, A. J. *Appl. Phys. Lett.* **1991**, *58*, 1982. (b) Cimrova, V.; Remmers, M.; Neher, D.; Wegner, G. *Adv. Mater.* **1996**, *8*, 146.
(22) (a) Scherf, U.; List, E. J. W. *Adv. Mater.* **2002**, *14*, 477. (b) Gaal, M.; List, E. J. W.; Scherf, U. *Macromolecules* **2003**, *36*, 4236.
(23) (a) Sims, M.; Bradley, D. D. C.; Ariu, M.; Koeberg, M.; Asimakis, A.; Grell, M.; Lidzey D. G. *Adv. Funct. Mater.* **2004**, *14*, 765. (b) Lee, J. I.; Klaerner, G.; Miller, R. D. *Chem. Mater.* **1999**, *11*, 1083.
(24) Bliznyuk, V. N.; Carter, S. A.; Scott, J. C.; Klarner, G.; Miller, R. D.; Miller, D. C. *Macromolecules* **1999**, *32*, 361.
(25) Blondin, P.; Bouchard, J.; Beaupré, S.; Belletête, M.; Durocher, G.; Leclerc, M. *Macromolecules* **2000**, *33*, 5874.
(26) Eaton, D. *Pure Appl. Chem.* **1998**, *60*, 1107.
(27) (a) Lu, J. P.; Tao, Y.; D'Iorio, M.; Li, Y. N.; Ding, J. F.; Day, M. *Macromolecules* **2004**, *37*, 2442. (b) Wong, W. Y.; Liu, L.; Cui, D.; Leung, L. M.; Kwong, C. F.; Lee, T. H.; Ng, H. F. *Macromolecules* **2005**, *38*, 4970.
(28) Janietz, S.; Bredley, D. D. C.; Grell, M.; Giebeler, C.; Inbasekaran, M.; Woo, E. P. *Appl. Phys. Lett.* **1998**, *73*, 2453.
(29) Hohle, C.; Hofmann, U.; Schloter, S.; Thelakkat, M.; Strohriegl, P.; Haarer, D.; Zilker, S. J. *J. Mater. Chem.* **1999**, *9*, 2205.

MA061770J